ac-susceptibility study of the 110-K superconducting phase of Bi-Sr-Ca-Cu-O

S. Ravi and V. Seshu Bai
School of Physics, University of Hyderabad, Hyderabad - 500 134, India
(Received 27 August 1993; revised manuscript received 26 January 1994)

ac-susceptibility (χ', χ'') measurements as a function of temperature and ac field amplitude have been carried out on cylindrical samples of the 110-K phase of the Bi-Sr-Ca-Cu-O system. The two single-phase samples used for studies were prepared under different experimental conditions with an aim to understand the regimes of validity of Bean's and Kim's critical-state models. Material-dependent parameters, such as critical current density as a function of temperature and effective volume fraction of grains, were estimated using these models. Improvements in the critical current density and intergrain coupling strength were found when a sample was subjected to intermediate cold pressing between sinterings. The field variation of the intergranular matrix susceptibility of the sintered sample could be fitted well to Kim's model whereas the data on the press sintered sample were in agreement with Bean's model.

I. INTRODUCTION

ac-susceptibility measurements on polycrystalline high-critical-temperature (high-T_c) superconductors not only facilitate an unambiguous determination of T_c onset of different phases, but also allow us to learn the nature of the coupling between the grains.[1,2] The real (χ') and imaginary (χ'') components of the ac susceptibility measured at low frequencies can be analyzed in terms of critical-state models.[3–7] According to Bean's[3] field-independent critical-state model, the critical current density (J_c) at a temperature (T_m) where $\chi''(T)$ exhibits an intergranular peak can be written as

$$J_c(T_m) = \frac{H_m}{a}, \tag{1}$$

where H_m is the ac field amplitude at the surface of a cylindrical sample and a is the radius. Subsequent to Bean's field-independent critical-state model, several field-dependent models for $J_c(H_i)$ were developed.[8–11] According to Kim's critical-state model, $J_c(H_i) = k/(H_0 + H_i)$, where H_i is the local internal field, and k and H_0 are positive constants. Expressions for magnetization and susceptibility have been derived using Kim's model for $J_c(H_i)$,[6,11–14] and also using modified Kim's critical-state models.[15–18]

From the temperature dependence of the ac susceptibility at different ac field amplitudes, $J_c(T)$ of polycrystalline $YBa_2Cu_3O_7$ samples were estimated[5,19] using Eq. (1) and Clem's[4] expressions derived from Bean's model. Also, $J_c(T)$ values have been estimated for a polycrystalline single-phase $YBa_2Cu_3O_7$ sample[7] and multiphase $Bi_{1.8}Pb_{0.2}Sr_2Ca_2Cu_3O_y$ compounds,[20] using susceptibility data and employing Kim's model. In the (Tl,Pb) $(Ba,Sr)_2Ca_2Cu_3O_y$ superconductor, Schilling *et al.*[21] have estimated the distribution of intergranular J_c and intergranular volume fraction from their ac-susceptibility data using an extended Bean model.

In the present work, to check the extent of validity of the theoretical expressions for susceptibility derived from Bean's and Kim's models, we have analyzed the field and temperature dependence of the ac susceptibility measured on two different samples of the 110-K phase of the Bi-Sr-Ca-Cu-O system, prepared in single-phase form. The two cylindrical samples used for the present study were prepared under different experimental conditions and correspondingly they differ in their nature of intergranular structure, χ''_{max} values, etc.

We have calculated the theoretical intergranular matrix susceptibility using the following equations,

$$\chi'_m = \frac{2}{\pi H_m}\int_0^\pi M_m(\theta)\cos(\theta)d\theta, \tag{2}$$

$$\chi''_m = \frac{2}{\pi H_m}\int_0^\pi M_m(\theta)\sin(\theta)d\theta, \tag{3}$$

where the magnetization $M_m(\theta)$ has been taken from the expressions derived by Chen and Goldfarb[12] using Kim's model, and H_m is the amplitude of the applied ac field. The calculated theoretical susceptibility is a function of H_m/H_p and p. H_p is the full penetration field at which $\chi''(H_m)$ exhibits a peak and p is a parameter related to inhomogeneity in the current path. According to Ref. 12,

$$H_p = H_0\,[(1+p^2)^{1/2} - 1], \tag{4}$$

$$p = \frac{(2ka)^{1/2}}{H_0}. \tag{5}$$

The experimental intergranular matrix susceptibility can be extracted from the measured susceptibility using the following equations,[7]

$$\chi' = -f_g + (1 - f_g)\chi'_m, \tag{6}$$

$$\chi'' = (1 - f_g)\chi''_m, \quad (7)$$

where f_g is the effective volume fraction of the grains, χ'_m and χ''_m are the components of the intergranular matrix susceptibility, and χ' and χ'' are those of the measured susceptibility. Equations (6) and (7) are valid only at temperatures well below the transition temperature, because close to the transition temperature, the grain susceptibility χ'_g is no longer equal to -1.

II. EXPERIMENTAL DETAILS

The samples were prepared with the composition $Bi_{1.2}Pb_{0.3}Sr_{1.5}Ca_2Cu_3O_y$. The details of sample preparation, x-ray diffraction, and microstructural studies have been reported in Ref. 22. The samples used in the present study were prepared from citrate precursors and were presintered twice at 800 °C for 12 h with an intermediate grinding. One sample in the form of a cylindrical pellet was annealed at 860 °C for 15 days before quenching to room temperature (sample A). Another sample (B) was prepared using the uniaxial-press sintering route reported by Asano *et al.*[23] It was first annealed at 860 °C for 5 days and was subjected to uniaxial cold pressing. The uniaxially pressed sample was again annealed at 860 °C for 5 days before quenching to room temperature.

The ac susceptibility was measured using a mutual inductance bridge operated at 33.0 Hz. The voltages induced across the secondaries were input to a dual-phase lock-in amplifier to measure simultaneously the real (χ') and imaginary (χ'') parts of the susceptibility. The phase angle of the lock-in amplifier was adjusted such that $\chi'' = 0$ at 12 K for a small applied field, and the same phase adjustment was maintained for the measurements carried out at higher fields. The temperature variation was achieved using a helium-exchange gas-filled cryostat made by APD, equipped with a temperature controller. The susceptibility data were collected using a computer after stabilizing the temperature. The data were collected in 0.5-K intervals close to the transition. Temperature was measured using a calibrated Si-diode sensor with an accuracy of better than 0.05 K.

The field variation of susceptibility was carried out at different temperatures by increasing the ac field amplitude in steps. For every cycle of field variation at a fixed temperature, the sample was first cooled in zero field through the transition temperature. Also, for each measurement of temperature variation at a particular ac field, the sample was first cooled in zero field through the transition.

The absolute values of χ' and χ'' have been determined using the expressions used by Murphy *et al.*[19] The filling factor of samples in the secondary coil was taken into account using a procedure described by Couach and Khoder.[24] We found that the values of $\chi'(T)$ were close to -1 at 12 K for low-field measurements. However, we multiplied the $\chi'(12\text{ K})$ data by a factor such that $\chi'(12\text{ K})$ was exactly equal to -1, and the same factor was used for the $\chi'(T)$ and $\chi''(T)$ measured at higher fields. Demagnetization corrections were applied to both the measured field and susceptibility.

III. RESULTS AND DISCUSSION

The samples A and B were single phase with lattice parameters $a \simeq b \simeq 5.4$ Å and $c \simeq 37.1$ Å from x-ray-diffraction measurements, and texture along the c axis of the unit cell was observed in press sintered sample B. The scanning electron microscope micrographs of fractured cross sections of the samples show that the sintered sample A is highly porous compared to the press sintered sample. The size of the grains is relatively smaller in the press sintered sample. The temperature variations of resistivity of the samples A and B are shown respectively in Figs. 1(a) and 1(b). The zero-resistivity temperatures are, respectively, 106.4 and 105.9 K. The resistivity at 300 K for the samples A and B are respectively 5.843 and 2.685 m Ω cm. Whereas the $T_c(0)$ of the press sintered sample is comparable with that of the sintered sample, its $\rho(300\text{ K})$ is almost half of that observed in the sintered sample.

A. Field dependence of susceptibility

The field variation of χ' and χ'' measured at temperatures 97.0, 76.5, and 56.0 K for samples A and B is plotted as a function of $\log_{10}(H_m)$ (see Figs. 2 and 3 below). At low fields, the values of $\chi'(H_m)$ are close to -1 and the values of $\chi''(H_m)$ are close to 0. At higher fields, the value of $\chi'(H_m)$ rises as a result of the transition of the intergranular matrix into the normal state. The $\chi''(H_m)$ exhibits a peak as a result of full penetration of the applied field into the intergranular region and the value of the full penetration field H_p increases as the temperature is reduced. The H_p values of the sample A at the above three temperatures are 95.3, 712, and 1738 A/m. At 56.0 K we could not get the complete χ'' curve because the

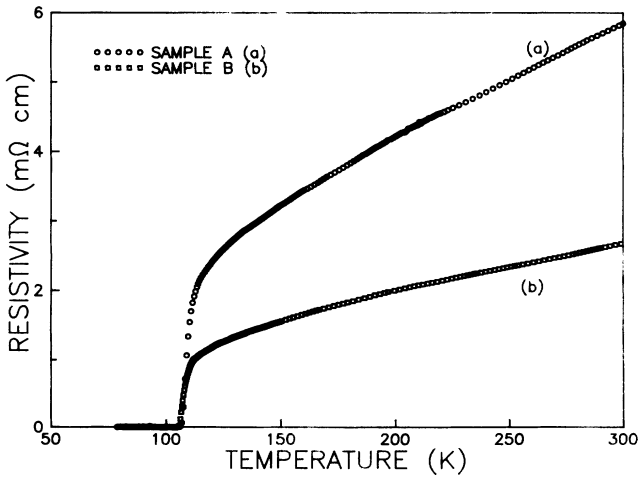

FIG. 1. Temperature variation of resistivity of the (a) sintered and (b) press sintered samples. The zero-resistivity temperatures are respectively 106.4 K and 105.9 K.

maximum field we can achieve with our experimental set up is limited to 2500 A/m. From the above experiments, we find that a comparatively larger field is needed for full penetration of flux in the press sintered sample compared to the sintered sample, at a given temperature. The H_p values obtained for samples A and B at different temperatures are given in Table I.

To determine the experimental intergranular matrix susceptibility (χ'_m and χ''_m) from Eqs. (6) and (7), we need to know the f_g value. To find the f_g value the following two conditions were used.[13] (1) The plot of $\log_{10}\chi''_m$ versus $\log_{10} H_m$ gives a peak of which both sides are almost linear. (2) χ''_m as a function of $-\chi'_m$ gives a convex curve with the slope $d\chi''_m/d(-\chi'_m)$ that tends to ∞ at $\chi'_m = 0$. By substituting tentative values for f_g in Eqs. (6) and (7), the values of $\chi'_m(H_m)$ and $\chi''_m(H_m)$ were calculated and were examined in the light of the above two conditions. Thus, the correct f_g values and corresponding $\chi'_m(H_m)$ and $\chi''_m(H_m)$ data were obtained at different temperatures. From the maximum matrix susceptibility $\chi''_{m,\max}$ and using Table I in Ref. 7, the parameter p was estimated at different temperatures. The values of H_0 and k were obtained using Eqs. (4) and (5). The estimated values of f_g, p, H_0, and k are given in Table I for samples A and B at different temperatures. The values of χ'_m and χ''_m at the full penetration fields are given in Table I. The ratio of the measured density of the sample to the x-ray density is taken as the volume fraction of the solid part of the material f_s, and it is respectively 0.51 and 0.79 for the samples A and B. From Table I we can see that the effective volume fraction of the grains f_g for sample A is very close to f_s. For the sample B, the f_g value is well below the f_s value.

As mentioned in the Introduction, Kim's susceptibility is a function of p and H_m/H_p. By substituting the above-determined p values, theoretical χ'_m and χ''_m values were calculated for different values of H_m/H_p. Figure 2 shows the plot of experimental (symbols) and theoretical (solid line) χ'_m and χ''_m as a function of $\log_{10}(H_m)$ for the sample A. In Fig. 2, we can see that the fit is good for all three temperatures.

In the case of the press sintered sample, the theoretical matrix susceptibility shows a considerable deviation from the experimental data, as can be seen from Fig. 3. At 97.0 K, the deviation from theory may be partly due to the inappropriate use of Eqs. (6) and (7) for the estimation of χ'_m and χ''_m, because at this temperature χ'_g will be no longer equal to -1. At 76.5 K, even though the χ''_m data are closer to theory, the χ'_m curve shows large deviation from theory. Moreover, we could not reproduce theoretically the χ' curve as a continuous one between low field ($H_m < H_p$) and medium field ($H_m > H_p$), as can be seen from Fig. 3, where the dash-dotted lines are an extrapolation of the low-field curve.

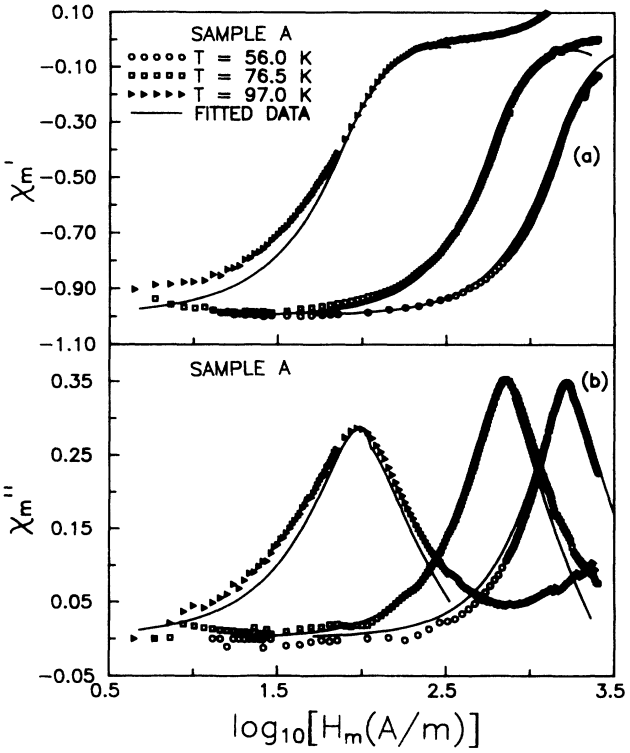

FIG. 2. Semilog plot of (a) real and (b) imaginary components of the intergranular matrix susceptibility as a function of ac field amplitude at the temperatures 56.0 K (circles), 76.5 K (squares), and 97.0 K (triangles), for the sintered sample (A). The solid lines are theoretical data calculated using Kim's model.

To fit the experimental data of sample B, we calculated the theoretical susceptibility using Bean's model. Bean's theoretical susceptibility was obtained using Eqs. (2) and (3) and taking the expressions for magnetization derived from Bean's model [Eqs. (82) and (83) in Ref. 12] for cylindrical samples. Bean's susceptibility is given as dashed lines in Fig. 3 and it gives a very good fit, especially at 76.5 K.

Kim's theoretical $\chi''_{m,\max}$ value can vary[7] from 0.21 to 0.4 for different values of p. In the present work, since the $\chi''_{m,\max}$ value observed in sample B is very close to the

TABLE I. List of parameters obtained from the field variation of susceptibility in samples A and B, where T is the temperature at which experiments were carried out.

Sample	T (K)	H_p (A/m)	$-\chi'_m(H_p)$	$\chi''_m(H_p)$	f_g	p	H_0 (A/m)	k (10^8A^2/m^3)
	56.0	1738	0.26	0.368	0.47	14.1	131.9	15.6
Sample A	76.5	712	0.285	0.351	0.47	9.5	83.1	28.1
	97.0	95.3	0.26	0.287	0.43	2.6	52.2	0.09
Sample B	76.5	1031	0.275	0.212	0.40	0.14	1.0×10^5	1070
	97.0	125.6	0.29	0.21	0.35	0.14	1.29×10^4	17.6

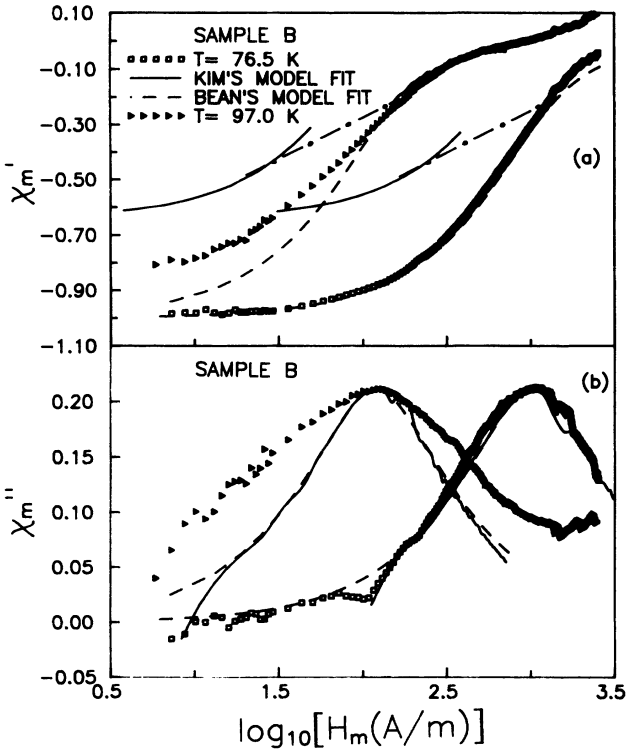

FIG. 3. Plot of (a) real and (b) imaginary components of the intergranular matrix susceptibility versus $\log_{10}(H_m)$, at the temperatures 76.5 K and 97.0 K for sample B. The solid lines are theoretical data calculated using Kim's model and the dash-dotted lines in the χ'_m versus $\log_{10}(H_m)$ plot are the extrapolation of Kim's low-field curve to medium field. The dashed lines are theoretical data calculated from Bean's model.

lower limit (0.21) of Kim's theoretical $\chi''_{m,\max}$, Kim's theoretical susceptibility shows considerable deviation from the experimental data. The values of $\chi''_{m,\max}$ observed in sample A are higher than 0.21 and its χ'_m and χ''_m data could be fitted well to Kim's theoretical susceptibility.

$\chi'(H_m)$ and $\chi''(H_m)$ were also measured on another sintered pellet of the 110-K superconductor prepared from nitrate precursors and analyzed using the above procedure. The $\chi'_m(H_m)$ and $\chi''(H_m)$ data of the nitrate-route pellet could be fitted well to Kim's theoretical susceptibility as in the case of sample A. Moreover, the values of f_g, H_p, and f_s for the nitrate-route pellet were comparable to those of sample A.

B. Temperature dependence of susceptibility

The temperature variation of the susceptibility measured at different ac field amplitudes, 23.9, 730, 1456, and 2189 A/m, is shown in Fig. 4 for sample A. The diamagnetic onset temperature is $\sim$ 107.5 K and it is almost constant at different fields. At higher fields the χ'' data show both the intergranular and intragranular peaks. The intergranular peak temperature T_m varies from 101.0 to 39.3 K, and the intragranular peak temperature T_g varies from 104.2 to 99 K, when the applied field amplitude is increased. From Fig. 4, we can see that the values of maximum $\chi''(T_m)$ are almost constant at higher fields. Using Eq. (1), and taking H_m as the field at which the experiment was carried out, the $J_c(T_m)$ values were estimated.

Similarly, the plots of $\chi'(T)$ and $\chi''(T)$ measured at different ac fields for the sample B are shown in Fig. 5. The diamagnetic onset temperature is 106.7 K. The magnitudes of the intergranular peak $\chi''(T_m)$ are almost constant at different applied higher fields. In contrast to the intergranular peak, the magnitude of the intragranular peak $\chi''(T_g)$ increases with applied field, for both samples studied. In sample B, the values of $\chi''(T_m)$ and $\chi''(T_g)$ are small compared to sample A and this could be as a result of finer particles in the press-sintered sample. The values of T_m, T_g, and $J_c(T_m)$ for the samples A and B are given in Table II.

To estimate the temperature variation of the critical current density $J_c(T)$ from the measured $\chi'(T)$ and $\chi''(T)$, we first estimated $\chi'_m(T)$ and $\chi''_m(T)$ from Eqs. (6) and (7). To determine $\chi'_m(T)$ and $\chi''_m(T)$, the value of f_g is needed, which was calculated from $\chi'(T)$ and $\chi''(T)$ as follows. The theoretical values of $\chi''_{m,\max}$ and $\chi'_m(\chi''_{m,\max})$ were calculated at $H_m = H_p$, for different values of p, using Kim's model. The theoretical values of $\chi''_{m,\max}$ and χ'_m at $\chi''_{m,\max}$ were substituted in Eqs. (6) and (7) in place of χ''_m and χ'_m, where χ' and χ'' are taken as the components of the measured susceptibility at T_m.

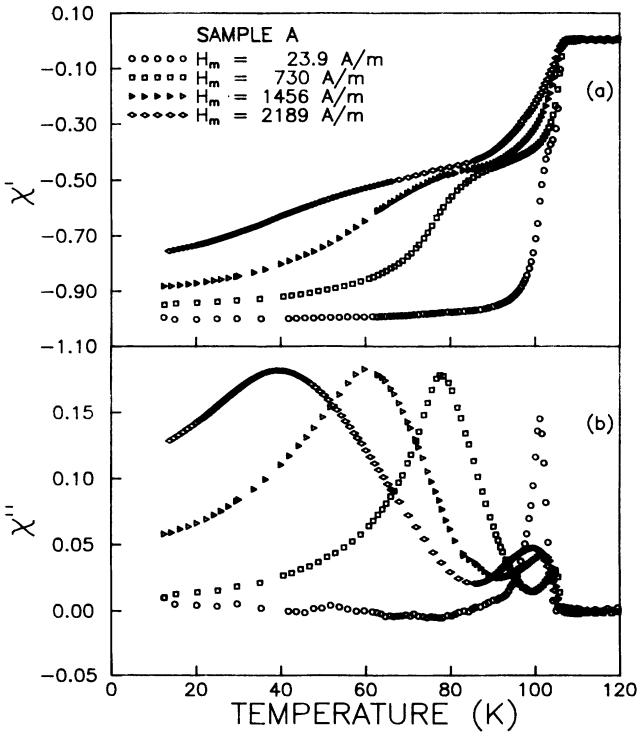

FIG. 4. Plot of (a) real and (b) imaginary components of the susceptibility versus temperature, measured in the sample A at ac field amplitudes 23.9 A/m, 730 A/m, 1456 A/m, and 2189 A/m.

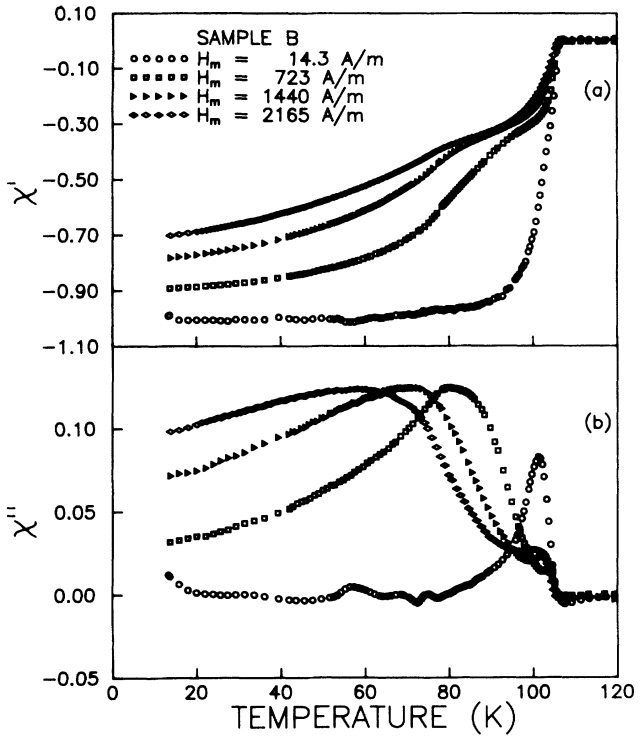

FIG. 5. The temperature variation of (a) real and (b) imaginary components of susceptibility measured in the press sintered sample (B) at ac field amplitudes 14.3 A/m, 723 A/m, 1440 A/m, and 2165 A/m.

The values of f_g derived from these two equations turn out to be unique only for a set of $\chi''_{m,\max}$ and χ'_m data calculated using a particular value of p, thus enabling a simultaneous estimation of p and f_g. Table II presents the p and f_g values obtained for the samples A and B. From Tables I and II, we find that the f_g values estimated from both the field and temperature dependences of the susceptibility are comparable.

The experimental values of $\chi'_m(T)$ and $\chi''_m(T)$ were calculated from $\chi'(T)$ and $\chi''(T)$ measured at a particular field (H_m), by substituting the values of f_g determined as above at T_m in Eqs. (6) and (7). The theoretical values of χ''_m as a function of H_m/H_p were calculated by substituting the value of p determined at T_m. By comparing the theoretical $\chi''_m(H_m/H_p)$ with experimental $\chi''_m(T)$ values, the full penetration fields $H_p(T)$ were determined and from these $J_c(T)$ were calculated using Eq. (1). Figure 6(a) shows the variation of $J_c(T)$ with temperature for sample A, at fields of 730, 1456, and 2189 A/m. The $J_c(T)$ values estimated at different fields are continuous as shown in Fig. 6(a). From the above-obtained $H_p(T)$ values and using Eqs. (4) and (5), the temperature dependence of Kim's constants H_0 and k were estimated and are shown in Figs. 6(b) and 6(c) for sample A.

Following the same procedure the temperature dependences of $J_c(T)$, $H_0(T)$, and $k(T)$ were estimated for sample B and are given in Fig. 7. From these plots we can observe that the $J_c(T)$ value is higher in the press-sintered sample. The H_0 and k values estimated for the press sintered sample are more than two orders of magnitude higher than that of the sintered sample and this indicates that the $J_c(H_i)$ of sample B is almost independent of field.

Since the data on sample B are found to give a better fit to Bean's model, we repeated the above calculations using Bean's theoretical susceptibility. The estimated values of $J_c(T)$ from Bean's model are shown as a solid line in Fig. 7(a). The $J_c(T)$ estimated from both models are comparable.

The f_g value can also be estimated from the field and temperature variation of χ'. In the plot of χ' versus $\log_{10} H_m$, the χ' value increases with the applied field and reaches an asymptotic value beyond a particular field, where the χ' is almost constant. If the field is further increased, the χ' value again increases, as can be seen in Figs. 2 and 3, especially at 97.0 K. The initial rise in χ' is due to the intergranular region and the second rise in χ' at higher field is due to the intragranular region. The value of $-\chi'$ in the asymptotic region will be equal to f_g at the particular temperature at which the experiment was carried out. Similarly, the temperature dependence of χ' at higher fields shows two different transitions corresponding to intergranular and intragranular regions as can be seen in Figs. 4 and 5. The value of $-\chi'$ at the temperature where the intergranular region just becomes normal is equal to f_g. The values of f_g obtained from χ' versus T and $\log_{10} H_m$ are comparable to that obtained from Eqs. (6) and (7) as described in Secs. III A and III B.

TABLE II. The list of parameters obtained from the temperature dependence of the susceptibility measured at different ac field amplitudes (H_m) for the samples A and B. T_m and T_g are inter- and intragranular χ'' peak temperatures.

Sample	H_m (A/m)	T_m (K)	T_g (K)	$J_c(T_m)$ (A/cm^2)	$-\chi'_m(T_m)$	$\chi''_m(T_m)$	f_g	p
	23.9	101.0		2.1				
Sample A	730	77.7	104.2	65.6	0.25	0.339	0.48	7.1
	1456	60.6	101.0	130.9	0.25	0.370	0.51	17.0
	2189	39.3	99.0	196.7	0.25	0.370	0.51	18.0
	14.3	101.0		1.55				
Sample B	722	80.0	103.8	78.1	0.255	0.215	0.42	0.34
	1440	70.6	102.2	166.0	0.19	0.215	0.42	0.23
	2165	58.3	100.0	234.4	0.19	0.214	0.42	0.23

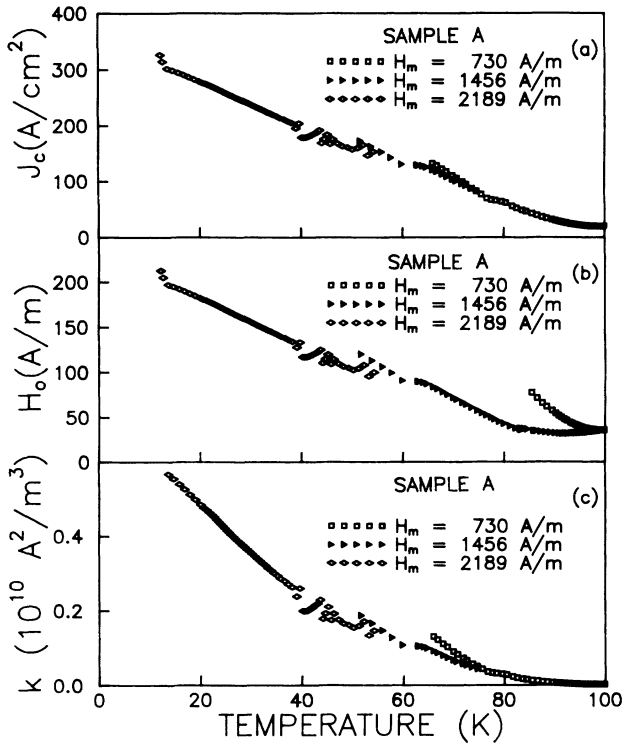

FIG. 6. Temperature variation of (a) critical current density (b) Kim's constant H_0, and (c) Kim's constant k, estimated by comparing the theoretical susceptibility calculated using Kim's model with the experimental susceptibility measured at the fields of 730 A/m, 1456 A/m, and 2189 A/m, in the sample A.

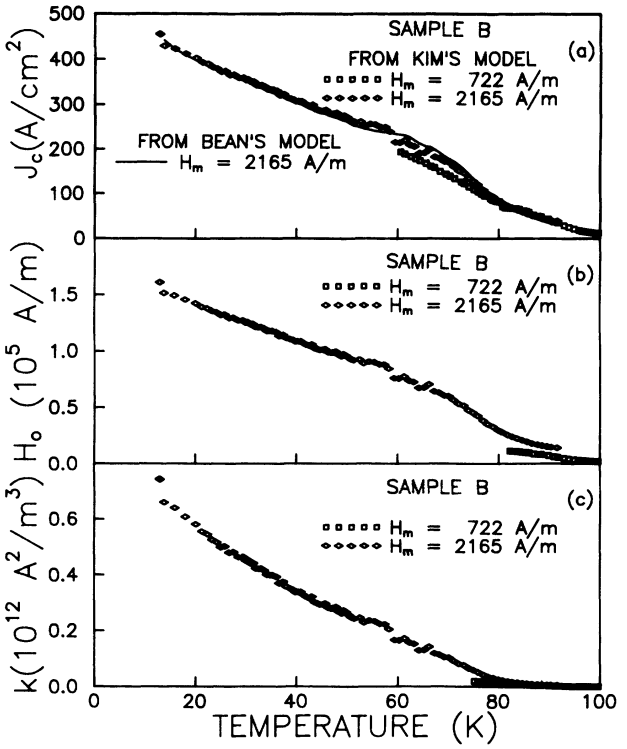

FIG. 7. Temperature variation of (a) critical current density and Kim's constants (b) H_0, and (c) k, estimated by comparing Kim's theoretical susceptibility with the experimental susceptibility of press sintered sample B at the fields 722 A/m and 2165 A/m. The solid line shows the plot of J_c versus T, estimated using Bean's theoretical susceptibility.

The decoupling field at which coupling between the grains is broken is calculated by extrapolating the plot of H_m versus T_m to T_m=0. The estimated decoupling fields are respectively 3580 and 5000 A/m for samples A and B. The press-sintered sample shows stronger coupling between the grains.

The $\chi'(T)$ and $\chi''(T)$ measured on another sintered pellet of the 110-K superconductor prepared from nitrate precursors were also analyzed using the above procedure. The estimated values of f_g, $J_c(T)$, and etc. are comparable to that of the sintered sample A.

IV. CONCLUSIONS

From a detailed analysis of the field and temperature dependences of the susceptibility in the 110-K phase of the Bi-Sr-Ca-Cu-O system, the following conclusions can be drawn. The field dependence of the susceptibility for the sintered pellet could be fitted well to the susceptibility derived from Kim's critical-state model. For the press sintered sample, whose $\chi''_{m,\max}$ data are close to 0.21, Kim's model shows considerable deviation from the experimental data. However, the susceptibility of the press-sintered sample could be fitted well to Bean's model. The values of effective volume fraction of the grains (f_g) estimated for the sintered sample were close to the volume fraction of the sample (f_s). In the press sintered sample the f_g values were well below the f_s value. The large difference between f_g and f_s is due to the smaller grains in the press sintered sample, where the flow of supercurrents on the surface of each of the small grains gives rise to a reduction in the effective volume fraction of the grains.

The $J_c(T)$ values estimated for both the samples are almost continuous. The press sintered sample exhibits increases in $J_c(T)$ values and also stronger coupling between the grains.

ACKNOWLEDGMENTS

The authors are thankful to Professor S. M. Bhagat for valuable discussions. This work is supported by the Department of Science and Technology (DST/NSP) and UGC-COSIST. S.R. gratefully acknowledges the Council of Scientific and Industrial Research (CSIR) for financial support.

[1] M. Nikolo and R.B. Goldfarb, Phys. Rev. B **39**, 6615 (1988).
[2] H. Mazaki, M. Takano, R. Kanno, and Y. Takeda, Jpn. J. Appl. Phys. **26**, L780 (1987).
[3] C.P. Bean, Rev. Mod. Phys. **36**, 31 (1964).
[4] J.R. Clem, Physica C **153-155**, 50 (1988).
[5] F. Gömory and P. Lobotka, Solid State Commun. **66**, 645 (1988).
[6] K.H. Müller, Physica C **159**, 717 (1989).
[7] D.X. Chen, J. Nogues, and K.V. Rao, Cryogenics **29**, 800 (1989).
[8] Y.B. Kim, C.F. Hempstead, and A.R. Strnad, Phys. Rev. **129**, 528 (1962).
[9] J.H.P. Watson, J. Appl. Phys. **39**, 3406 (1968).
[10] F. Irie and K. Yamafuji, J. Phys. Soc. Jpn. **23**, 255 (1967).
[11] W.A. Fietz, M.R. Beasley, J. Silcox, and W.W. Webb, Phys. Rev. **136**, A335 (1964).
[12] D.X. Chen and R.B. Goldfarb, J. Appl. Phys. **66**, 2489 (1989).
[13] D.X. Chen, A. Sanchez, T. Puig, L.M. Martinez, and J.S. Muñoz, Physica C **168**, 652 (1990).
[14] K. Yamamoto, H. Mazaki, and H. Yasuoka, Phys. Rev. B **47**, 915 (1993).
[15] M.C. Ohmer and J.P. Heinrich, J. Appl. Phys. **44**, 1804 (1993).
[16] L. Ji, R.H. Sohn, G.C. Splading, C.J. Lobb, and M. Tinkham, Phys. Rev. B **40**, 10 936 (1989).
[17] Y. Kim, Q.H. Lam, and C.D. Jeffries, Phys. Rev. B **43**, 11 404 (1991).
[18] Q.H. Lam, Y. Kim, and C.D. Jeffries, Phys. Rev. B **42**, 4846 (1990).
[19] S.D. Murphy, K. Renouard, R. Crittenden, and S.M. Bhagat, Solid State Commun. **69**, 367 (1989).
[20] D.X. Chen, Yu Mei, and H.L. Luo, Physica C **167**, 317 (1990).
[21] O.F. Schilling, K. Aihara, A. Soeta, T. Kamo, and S. Matsuda, Phys. Rev. B **47**, 8096 (1993).
[22] V. Seshu Bai, S. Ravi, T. Rajasekharan, and R. Gopalan, J. Appl. Phys. **70**, 4378 (1991).
[23] T. Asano, Y. Tanaka, M. Fukutomi, K. Jikihara, J. Machida, and H. Maeda, Jpn. J. Appl. Phys. **27**, 1652 (1988).
[24] M. Couach and A.F. Khoder (unpublished).